

TSUNAMI EVENT IDENTIFIED IN A SEDIMENTARY RECORD OF THE GAZA STRIP, PALESTINE

Khalid Fathi Ubeid

Department of Geology, Faculty of Science, Al Azhar University-Gaza, P.O. Box 1277, Gaza Strip, Palestine;
<https://orcid.org/0000-0002-9927-6597>; e-mail: khubeid@hotmail.com; k.ubeid@alazhar.edu.ps

Abstract:

The outcrop of the tsunami deposits, about 6 m thick, is located in the archaeological site Tel Askan in the Al Zhraa locality, southwest of the Gaza City. These deposits are unconformably underlain by sand dunes and sharply overlain by a palaeosol. They are pale gray sands mixed with volcanic ash and fine-grained deposits, and are intercalated with peat, few centimetres thick. The sand-sized grains are well rounded and well sorted, and consist mainly of quartz and subordinate of feldspar. Both macro- and microfossils were observed from tsunami deposits. Additionally, rip-up clasts and pottery shards were observed, indicating higher-flow regime. The potteries in tsunami deposits provide evidence for tsunami inundation at distance of about 1 km from the present shoreline.

sq

Key words: tsunami, sedimentology; pottery shard, rip-up clast; Gaza Strip

Manuscript received 26 December 2020, accepted 25 February 2021

INTRODUCTION

Tsunamis are among of the most dangerous fast-paced threats affecting coastal population centres and economic infrastructure (Morton *et al.*, 2007). By using data from past events, an understanding of how often they occur and their scale potential is facilitated (e.g. Salamon *et al.*, 2007; Yolsal *et al.*, 2007). Tsunami catalogues are assembled based on historical documents, witness reports and field data (Papadopoulos *et al.*, 2014); and there is a decrease in a number of occurrences reported each century due to limitation of written and instrumentally recorded records closer to the present, as the catalogue goes back in time (Goodman-Tchernov *et al.*, 2016). Modern tsunami field description have resulted in a better understanding of the sedimentological signatures left behind in the aftermath of a tsunami (e.g. Jaffe *et al.*, 2003; Goto *et al.*, 2011, 2012; Bahlburg and Spiske, 2012; Aránguiz *et al.*, 2016). Through contrasting these modern analogues, a new knowledge has increased the ability to identify older events in a sedimentary record. Nevertheless, these modern deposits are usually described in the first weeks, months and years after the initial event, while decades, centuries or more can pass before field events are described. Modern descriptions therefore cannot fully account for the taphonomic changes occurring in older deposits, but they provide a baseline from which past deposits can be analyzed and interpreted.

Usually, a detection of an anomalous sedimentary horizon as a tsunamite is achieved by contrasting the suspected

deposit with known tsunamigenic indicators, showing that the deposit does not comply with other transport mechanisms such as storms and floods, and agreeing to a historical record (if available). Comparisons of non-tsunamigenic deposits with recognized tsunamites within the same study area provided useful examples to direct the distinction between various depositional scenarios (e.g., Goff *et al.*, 2004; Kortekaas and Dawson, 2007; Morton *et al.*, 2007; Phantuwongraj and Choowong, 2012; Pilarczyk *et al.*, 2014; Sakuna-Schwartz *et al.*, 2015). One way to solve this was by coastal boulder deposit evaluations (Shah-Hosseini *et al.*, 2013). Tsunamis were shown to move large boulders during tsunami events (Scheffers, 2002; Goto *et al.*, 2010; Paris *et al.*, 2010; Scheucher and Vortisch, 2011), while storms were also shown to have the ability to dislodge and cause boulder movement depending on the relative roughness of the underlying surface and wave characteristics (Weiss, 2012; Zainali and Weiss, 2015) though storm moved boulders result in more orderly boulder fields while tsunami transported boulders are less organized. Although a proxy toolbox may be used to assess whether a deposit qualifies as tsunamigenic, the applicability varies widely depending on the specific environment of the site (e.g. Dominey-Howes, 2007; Bruins *et al.*, 2008; Chagué-Goff, 2010; Goff *et al.*, 2012; Pilarczyk *et al.*, 2014; Nelson *et al.*, 2015).

The tsunamis deposits are a valuable source of information for geologists and emergency planners. Therefore, in this paper the tsunami events examined in a sedimentary record in the Gaza Strip would be the first work in this

area. The selected field site is named Tel Askan and is located in the Al Zhraa locality to the southwest of the Gaza City in the Gaza Strip, in which the tsunami deposits and archaeological outcrop were formed by excavation works. Tel Askan is one of the most prominent archaeological sites in the area, and was a dominant coastal locality throughout the Antiquity. It is one of the oldest Phoenician sites dated at 6000–4000 BC (Negev and Gibson, 2001). First occurrences were accidentally discovered while excavating for foundations of a residential complex in 1998.

GEOGRAPHICAL AND GEOLOGICAL BACKGROUND

The Gaza Strip is located at the southern part of Palestine’s Mediterranean coast, approximately 12 km south of Ashkelon (Fig. 1). The coastal plain contains parallel shore aeolian ridges (locally termed Kurkar ridges) that generally extend in the NNE-SSW direction. The surface elevation ranges from the mean sea level to approximately 110 m a.s.l. The depressions, which contain alluvial deposits, are approximately 20–40 m a.s.l. (Ubeid, 2010, 2016). The dominant source for sediment is the Nile River. Its moderately well sorted quartz sand is moved by a long-shore transport in a northerly direction (Klein, *et al.*, 2007; Zviely *et al.*, 2007; Ubeid, 2011; Ubeid and Albatta, 2014; Ubeid and Ramadan, 2017). The area has a rich catalogue of earthquakes and tsunami events (e.g. Ambraseys and Karcz, 1992; Ambraseys *et al.*, 1994; Amiran, 1994; Soloviev *et al.*, 2000; Fokaefs and

Papadopoulos, 2007; Altinok *et al.*, 2011; Salamon *et al.*, 2011, 2007; Papadopoulos *et al.*, 2014). Within these tsunami catalogues, the Gaza Strip is associated with events that occurred in 1032, 1068, 1546, and possibly 1759 AD (Maramai *et al.*, 2014). Past studies suggested that there were coastal tsunami deposits from the Bronze Age eruption of Santorini, though the deposits of which have been neither dated nor analysed in detail (Pfannenstiel, 1960). The tsunamis in this region are presumably initiated by landslides and submarine slumping triggered by near and far field earthquakes and volcanic eruptions; such as those originating in the Cypriot and Aegean arcs (e.g. Fokaefs and Papadopoulos, 2007; Salamon *et al.*, 2007; Yolsal *et al.*, 2007; Katz *et al.*, 2015).

MATERIALS AND METHODS

Field Procedure

A classical field work survey was conducted aimed at identifying anomalous, possibly tsunamigenic horizons along the eroded coastline of the Gaza Governorate, and focusing at the Al Zhraa locality (Fig. 1) where the excavation work shows some features in deposits expected to attribute to ~3.5 ka Santorini eruption (Pfannenstiel, 1952, 1960; Friedrich *et al.*, 2006), and a natural alluvial deposit (Rosen, 2008). Identified sections were cleaned, described and photographed, and rock samples, potteries, shells and organic remains were collected to be used for comparison with the sediments from the coastal section.

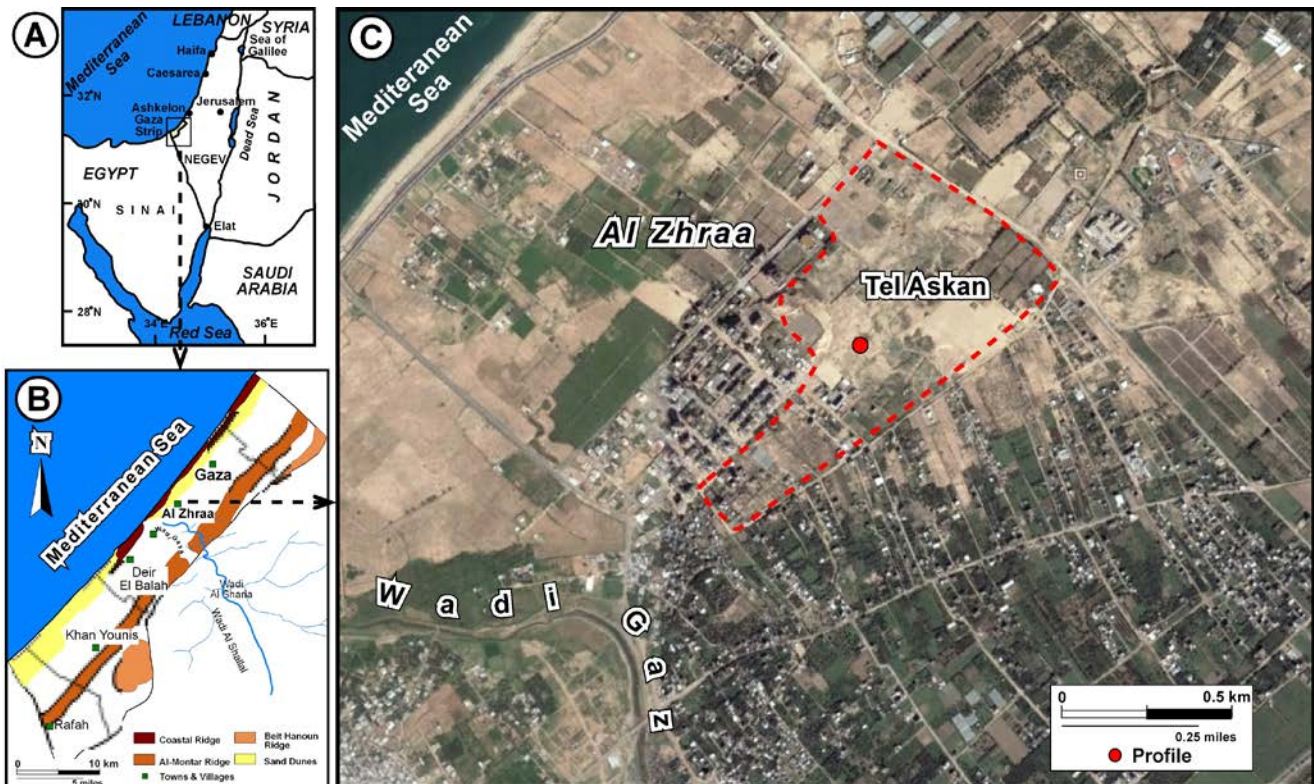


Fig. 1. Location map of a research area; the red polygon shows a layout of the archaeological site (Tel Askan).

Laboratory analysis

In order to clarify the field observations, laboratory analysis was done. Initially, the samples were dried at 110°C in an oven for a complete removal of moisture. Sedimentation method, using hydrometer and dispersive calgon, was applied to separate grain sizes for each fine-grained sample. In order to identify physical properties and mineral composition of the sand grains, sand-sized fractions were separated from finer particles using US mesh sieve #200. The Olympus binocular microscope was used to study grain morphology, in addition to fossils and bioclast contents.

RESULTS AND DISCUSSION

An onshore profile was collected from an outcrop excavated to the southwest of the Gaza City (about 800 m to the east from the beach) (Fig. 1). The studied section is at 30 m a.s.l. It consists of three tsunami units, composed of sand mixed with silt, clay and volcanic ash. It was intercalated with peat, few centimetres thick. It is unconformably underlain by aeolian sand and sharply overlain by a palaeosol (locally termed Hamra) (Figs 2 and 3). The underlying friable aeolian sand is fine- to medium grained and highly resembles the beach sand documented earlier (Ubeid, 2010, 2011;

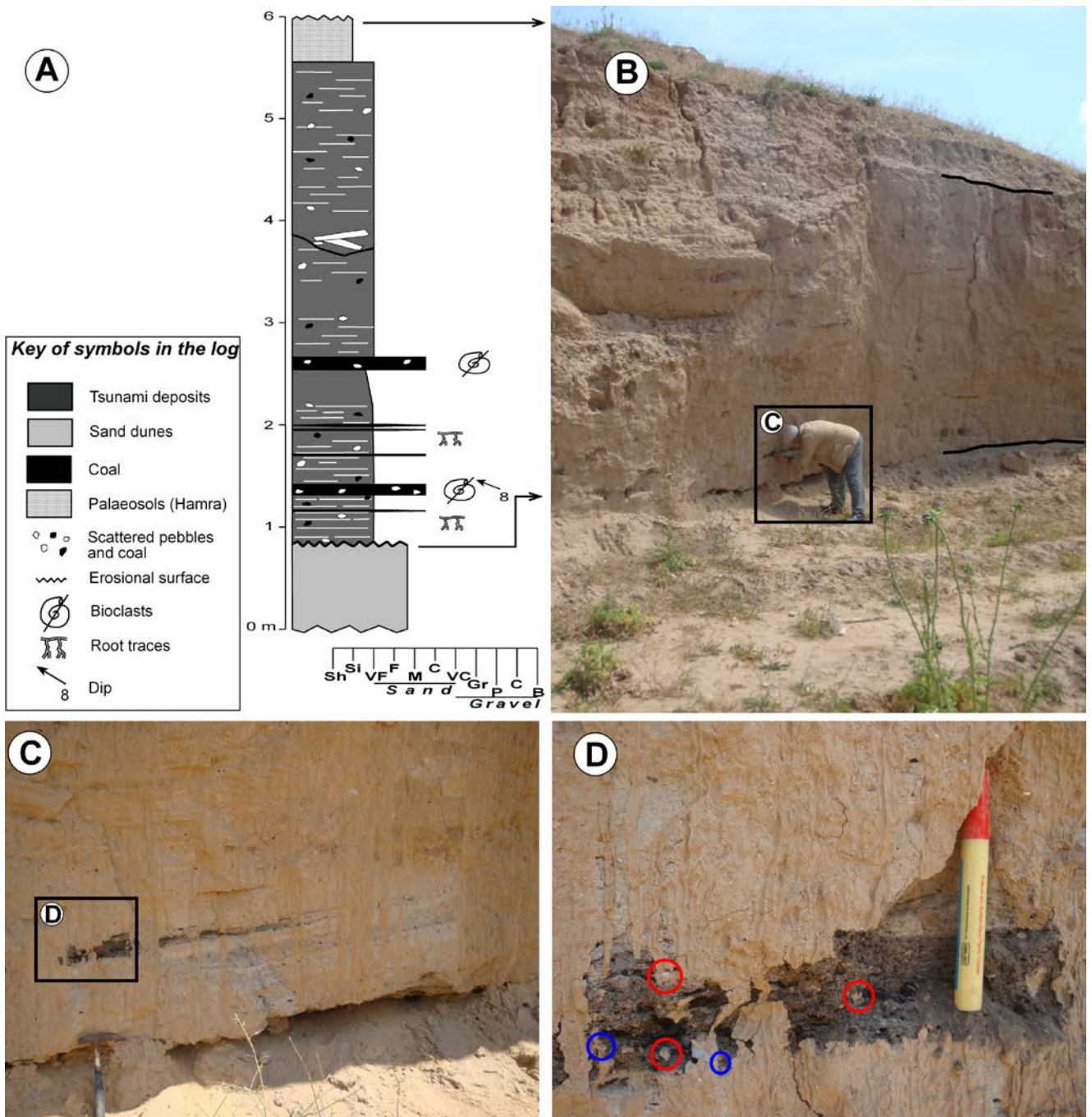


Fig. 2. (A) stratigraphic section with the sedimentary succession in the profile, (B) coastal archaeological site of Gaza Strip, (C) erosional surface between the tsunami deposits and the sandy dunes, (D) intercalated coal in the tsunami deposits (red circles – pebbles, blue circles – bioclasts).

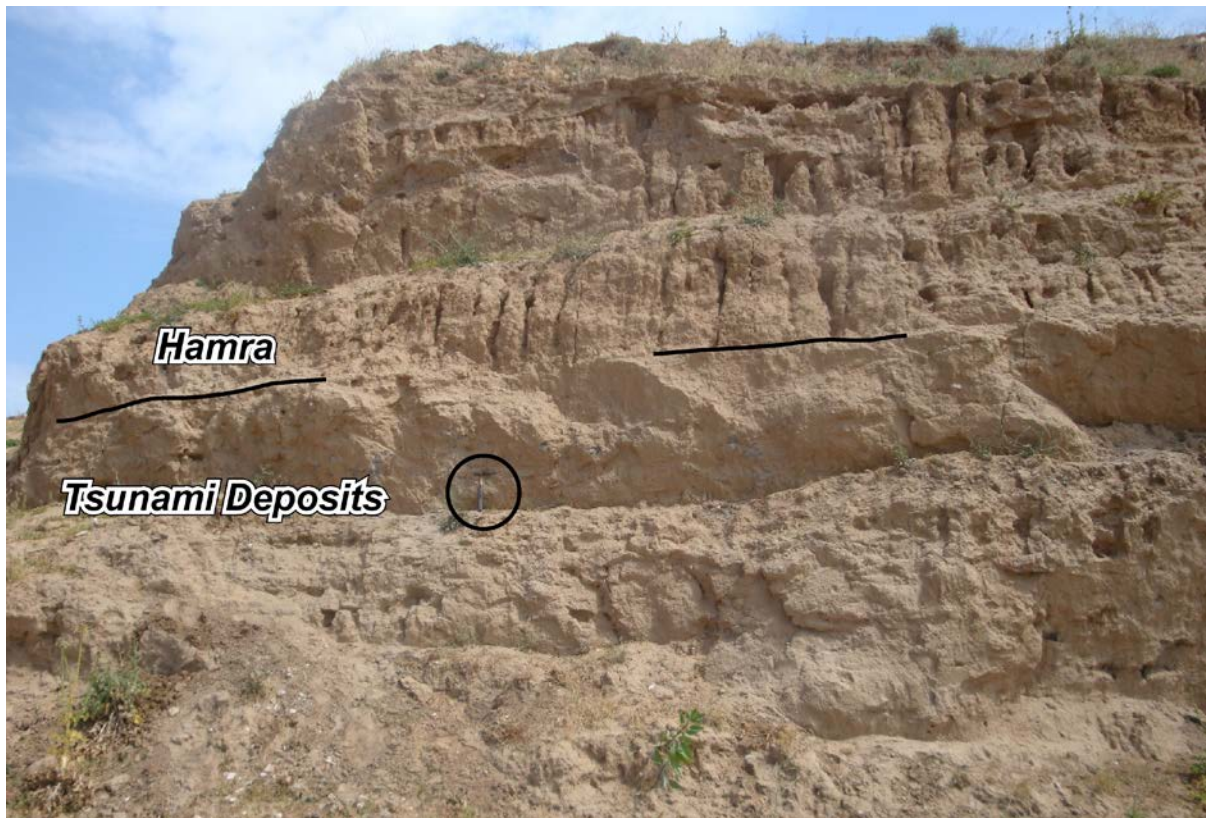


Fig. 3. Tsunami deposits sharply overlain by the Hamara palaeosol.

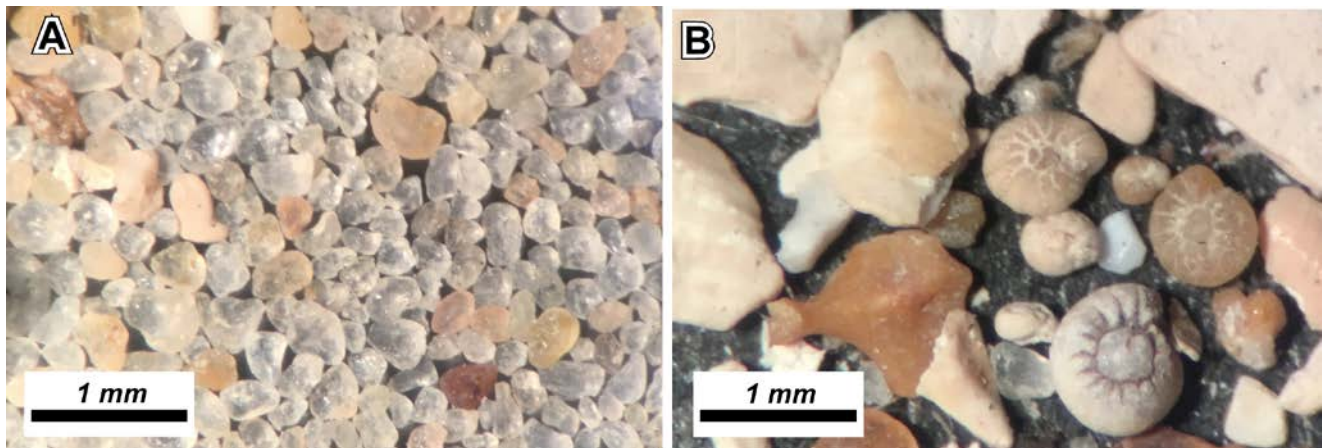


Fig. 4. Microscopic photographs: (A) grain shape and composition, (B) microfossils and carbonate bioclasts.

Ubeid and Albatta, 2014; Ubeid and Ramadan, 2017; Ubeid *et al.*, 2018). The overlying palaeosol is composed of reddish-brown fine-grained to very fine sand, silt and clay, with scattered small- to medium size pebbles and snail shells.

The deposits of tsunami units are distinguished from the other deposits in the sequence by their pale grey colour as well as Kurkar and Hamra deposits in the Gaza Strip. Overall, the grain-size analysis of these units proved that they are composed of about sand (57%), silt (32%) and clay (11%). The sand of these units consists of rounded- to well-rounded and well sorted fine- to very fine grains. They are

mainly composed of quartz with subordinate amount of feldspars (Fig. 4A).

Thickness and geometry

The lower unit (unit 1) is up to 2 m thick. Its erosional base overlays the aeolian sand and it is gradationally underlain by the second unit (unit 2) (Fig. 2). The unit 2 is about 1.5 m thick and sharply overlies the Hamra palaeosol (Fig. 3). It is planar in shape and dips about 10° towards the



Fig. 5. Lenticular tsunami deposits unit 3 and slumping boulders of these deposits; dashed line shows the erosional surface.

west. The lower part of these laminated units pass upwards into massive with rip-up clasts, shells, bioclasts and spots of dispersed peat. The laminae are from 1 to 5 cm thick and pinch out eastwards. Intercalated peat deposits were observed in these units.

The third unit (unit 3) is located some metres eastwards of the previous units. It is diagnostically lenticular in shape, with a concave base and a flat top (Fig. 5). It is erosionally underlain by the unit 2 with slumping boulders and overlain by the Hamra palaeosol with lenses of conglomerates. The maximum thickness of this unit is about 2 m. The unit is massive and consists of fine-grained sand, mixed with volcanic ash. It contains scattered fossils, pebbles and pottery shards with no preferred orientation.

The sedimentary contacts in the succession are important, because they indicate changes in the sedimentation pattern. The abrupt basal contacts indicate a rapid change in the depositional pattern consistent with sudden influx of the tsunami sediments. Upper contacts which range from gradual to abrupt reflect patterns of the post tsunami deposition.

Fossils

Both macrofossils and microfossils were found in the tsunami deposits. The microfossils were composed mainly

of fine- to medium carbonate bioclasts and subordinate foraminifera fossils (Fig. 4B). Most of the foraminifera were yellow stained. Macrofossils consist of marine mollusks, mainly bivalve types, in addition to bones of vertebrates and various plant fossils (Fig. 6A–B). The bivalves in the unit 1 and the unit 2 were oriented, while they were chaotic in the unit 3. Overall, presence of marine and brackish organic remains in water and scattered bioclasts shells provide evidence for marine incursion. Yellow foraminifera and bioclasts are present throughout the deposits, and were recorded in other tsunami deposits as well as are a part of corrosion features (Pilarczyk *et al.*, 2014; Goodman-Tchernov *et al.*, 2016).

Peat

Peat deposits observed in the unit 1 and the unit 2 form relatively small lenses, tens of metres long and maximum 10 cm thick. They contain coarse material e.g. coarse sand, small pebbles and fragments of Hamra (Figs 2D and 6A–C). However, the peat deposits refer to a tidal marsh sedimentation, in which peat develops from subaerially exposed, well-vegetated marsh soils in the intertidal zone. The spots of peat in the upper part of the unit 1 suggest that the tsunami flow eroded some peat (Moore *et al.*, 2007; Peters *et al.*, 2007).

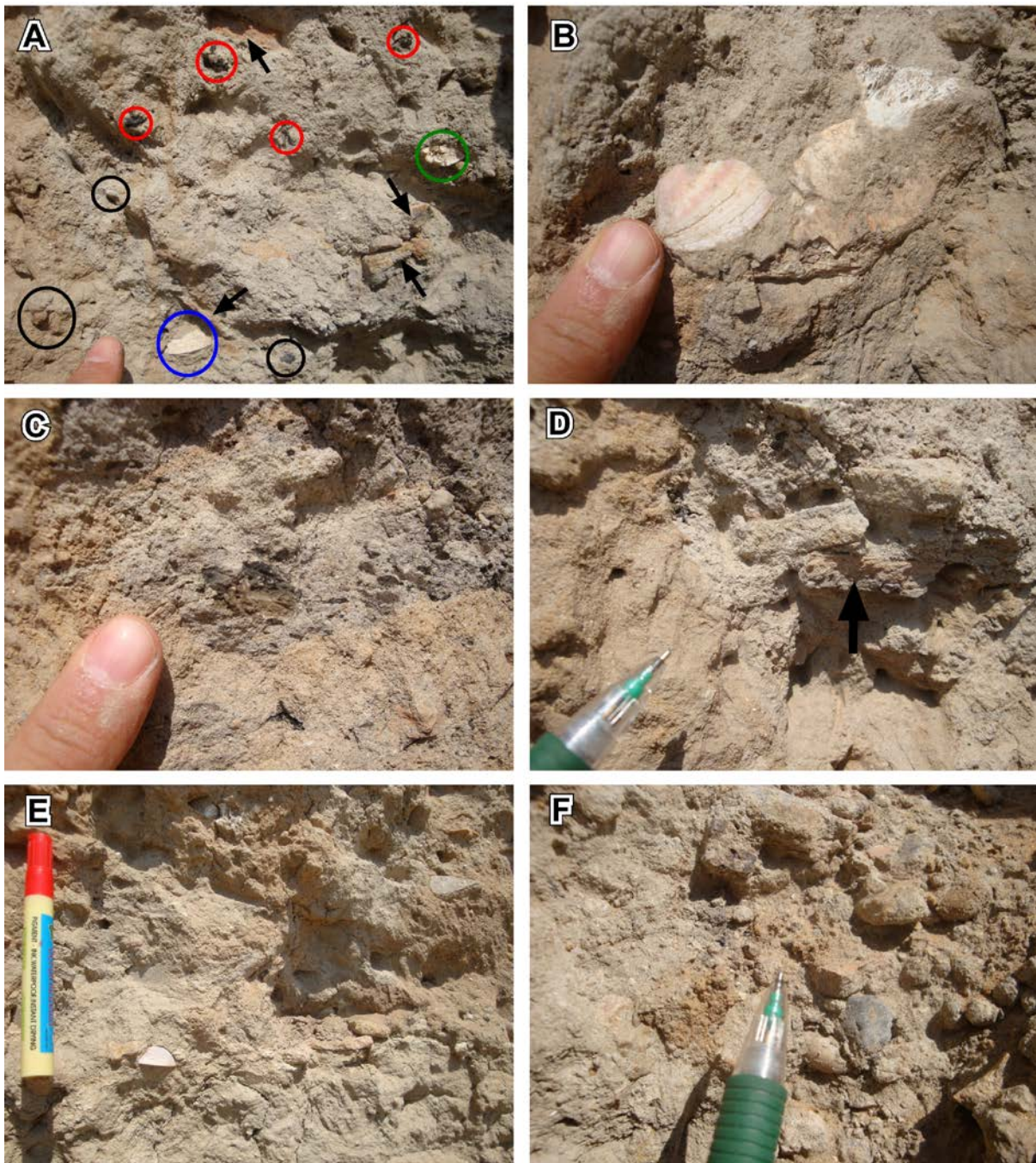


Fig. 6. Tsunami deposits content: (A) general view with bivalves, bones of invertebrates (marked by blue and green circles respectively), peat of plant remains (marked by red circles), rip-up clasts (marked by black circles) and pottery clasts (marked by black arrow); (B) bivalves and bones of invertebrates in tsunami deposits; (C) peat (black colour); (D) pottery clasts; (E) oriented shells and pottery clasts indicate a low-flow regime; (F) chaotic rip-up clasts and potteries indicate high-flow regime.

Pottery shards and rip-up clasts

The units of the tsunami deposits were dominated by flat-lying pottery. These shards can be assigned to the 4–5 century BC (Negev and Gibson, 2001; Hoffmann *et al.*, 2018). They were imbricated in the lower parts of the unit 1 and the unit 2, oriented to the west, suggesting a palaeoflow direction of the tsunami (Fig. 6E). They are chaotic in the upper part, especially in the unit 3 with no preferred orien-

tation. The pottery shards indicate high-energy of tsunami and provide evidence for marine incursion. The flat-lying pottery, in addition to the imbricated shells in the units 1 and 2, were reported in the tsunami-derived deposits identified offshore at Ashqelon and Caesarea (for location see Fig. 1) (Goodman-Tchernov *et al.*, 2009; Hoffmann *et al.*, 2018).

Rip-up clasts are usually composed of pebbles and cobbles of silica, Hamra palaeosol and peat (Fig. 6F). They indicate high-energy and also suggest that the material was

not overwhelmed for long periods, enough to break apart the material into individual grains. These materials are previously described from turbidites, channel surges, subaquatic dunes and bars and tsunami deposits (Morton *et al.*, 2007). Boulder-size fragments with no preferred orientation were observed in the unit 3, indicating to channel rock collapse (Scheffers, 2002; Goto *et al.*, 2010; Paris *et al.*, 2010).

Overall, these rip-up clasts in the lower part and in the western part of the section and particularly flat-lying pottery shards imbrication, in addition to lamination in the lower parts of the units 1 and 2 clearly indicate a high-flow regime. On the other hand, the chaotic rip-up clasts in the unit 3 suggest hyper-concentrated flow, caused by the catastrophic effect of a strong tsunami.

In sense of Hoffmann *et al.* (2018) the pottery shards in their study area at Tel Tel Ashkelon, located to the north of the Gaza Strip provide a terminus post quem of around 5–4 century BC. At that time, sea level indicators suggest a similar sea-level as today (Sivan *et al.*, 2001, 2004; Lambeck *et al.*, 2014; Goodman-Tchernov and Katz, 2016). Due to coastal erosion and cliff retreat, coastal geomorphology has changed dramatically in recent years, as described above (Katz and Mushkin, 2013; Barkai *et al.*, 2017). Consequently, in this study the rip-ups of the Hamra palaeosol combined with pottery shards which were eroded by high energy current flow of the tsunami, suggest that the sea was further west than its present shore, meaning that the deposits within this study were even further inland relative to today.

Run-up and inundation distance

Run-up is defined as the elevation of the tsunami relative to sea level at maximum inundation and inundation distance farthest inland of tsunami penetration. However, studies of modern tsunamis document that the maximum elevation reached by a tsunami and the maximum extent of inundation is often beyond the maximum extent of sedimentation and sedimentation may be discontinuous near the limit of inundation (Gelfenbaum and Jaffe, 2003; Jaffe *et al.*, 2003). The eroded zone may also underestimate the run-up and inundation distance. Therefore, the highest recorded elevation and farthest distance inland of tsunami deposits is found to represent a minimum estimate of the run-up and inundation distance of the tsunami (Peters *et al.*, 2007).

The pottery shards in tsunami deposits provide evidence for tsunami inundation for about 1 km in the coastal zone from the present shoreline. The elevation of the coastal ridge at the studied section is about 30 m a.s.l. This indicates that a maximum overtopped by the tsunami inundation is about 30 m at about 1 km inland in the open coast and may be found more than this distance up wadis. This estimation of height elevation of inundation supposed that neither uplift nor subsidence occurred subsequent to a tsunami. Coastal uplift or subsidence that occurred during the time between deposition and elevation measurements of the deposit or barrier may have a significant effect on run-up determinations from paleotsunami deposits. In regions

where uplift or subsidence estimation rates are known, correcting for coastal uplift or subsidence improves run-up estimates (Peters *et al.*, 2007).

CONCLUSIONS

An anomalous depositional sequence found in ancient the Gaza City's Mediterranean shoreline has specific waterborne characteristics and may fit tsunamigenic criteria. Physical characteristics of tsunami deposits recognized in this study are: lamination of sand mixed with fine-grained deposits and volcanic ash, including rip-up clasts, foraminifera and pottery clasts.

The results show how sedimentological records can be valuable for understanding the history of a cultural heritage site within archaeological areas, expanding the tsunami catalogue. Ancient, natural, anomalous coastal deposits of uncertain origin may also be worth reconsidering in the context of better understanding of sedimentological indicators related to a tsunami.

Acknowledgements

Thanks are given to Mr. Jehad El-Shrqawi for his help in the fieldwork.

REFERENCES

- Altinok, Y., Alpar, B., Özer, N., Aykurt, H., 2011. Revision of the tsunami catalogue affecting Turkish coasts and surrounding regions. *Natural Hazards and Earth System Sciences* 11, 273–291.
- Ambraseys, N., Karcz, I., 1992. The earthquake of 1546 in the Holy Land. *Terra Nova* 4, 254–263.
- Ambraseys, N., Melville, C.P., Adams, R.D., 1994. *The Seismicity of Egypt, Arabia and the Red Sea: A Historical Review*. Cambridge University Press, pp. 181.
- Amiran, D.H., 1994. Location index for earthquakes in Israel since 100 BCE. *Israel Exploration Journal* 46, 120–130.
- Aránguiz, R., González, G., González, J., Catalán, P.A., Cienfuegos, R., Yagi, Y., Okuwaki, R., Urra, L., Contreras, K., Del Rio, I., Rojas, C., 2016. The 16 September 2015 Chile tsunami from the post-tsunami survey and numerical modeling perspectives. *Pure and Applied Geophysics* 173, 333–348.
- Bahlburg, H., Spiske, M., 2012. Sedimentology of tsunami inflow and backflow deposits: key differences revealed in a modern example. *Sedimentology* 59, 1063–1086.
- Barkai, O., Katz, O., Mushkin, A., Goodman-Tchernov, B.N., 2017. Long-term retreat rates of Israel's Mediterranean sea cliffs inferred from reconstruction of eroded archaeological sites. *Geoarchaeology* 1–14.
- Bruins, H.J., MacGillivray, J.A., Synolakis, C.E., Benjamini, C., Keller, J., Kisch, H.J., Klügel, A., van der Plicht, J., 2008. Geoarchaeological tsunami deposits at Palaikastro (Crete) and the Late Minoan IA eruption of Santorini. *Journal of Archaeological Science* 35, 191–212.
- Chagué-Goff, C., 2010. Chemical signatures of palaeotsunamis: a forgotten proxy? *Marine Geology* 271, 67–71.
- Dominey-Howes, D., 2007. Geological and historical records of tsunami in Australia. *Marine Geology* 239, 99–123.

- Fokaefs, A., Papadopoulos, G.A., 2007. Tsunami hazard in the Eastern Mediterranean: strong earthquakes and tsunamis in Cyprus and the Levantine Sea. *Natural Hazards* 40, 503–526.
- Friedrich, W.L., Kromer, B., Friedrich, M., Heinemeier, J., Pfeiffer, T., Talamo, S., 2006. Santorini eruption radiocarbon dated to 1627–1600 BC. *Science* 312, 548.
- Gelfenbaum, G., Jaffe, B., 2003. Erosion and sedimentation from the 17 July 1998 Papua New Guinea tsunami. *Pure and Applied Geophysics* 160, 1969–1999.
- Goff, J., Chagué-Goff, C., Nichol, S., Jaffe, B., Dominey-Howes, D., 2012. Progress in palaeotsunami research. *Sedimentary Geology* 243–244, 70–88.
- Goff, J., McFadgen, B.G., Chagué-Goff, C., 2004. Sedimentary differences between the 2002 Easter storm and the 15th-century Okoropunga tsunami, southeastern North Island, New Zealand. *Marine Geology* 204, 235–250.
- Goodman-Tchernov, B., Katz, T., Shaked, Y., Qupty, N., Kanari, M., Niemi, T., Agnon, A., 2016. Offshore evidence for an undocumented tsunami event in the “low risk” gulf of Aqaba-Eilat, Northern Red Sea. *PLoS One* 11, e0145802.
- Goodman-Tchernov, B., Katz, O., 2016. Holocene-era submerged notches along the southern Levantine coastline: punctuated sea level rise? *Quaternary International* 401, 17–27.
- Goodman-Tchernov, B.N., Dey, H.W., Reinhardt, E.G., McCoy, F., Mart, Y., 2009. Tsunami waves generated by the Santorini eruption reached Eastern Mediterranean shores. *Geology* 37, 943–946.
- Goto, K., Chagué-goff, C., Goff, J., Jaffe, B., 2012. The future of tsunami research following the 2011 Tohoku-oki event. *Sedimentary Geology* 282, 1–13.
- Goto, K., Kawana, T., Imamura, F., 2010. Historical and geological evidence of boulders deposited by tsunamis, southern Ryukyu Islands, Japan. *Earth-Science Reviews* 102, 77–99.
- Goto, K., Takahashi, J., Oie, T., Imamura, F., 2011. Remarkable bathymetric change in the nearshore zone by the 2004 Indian Ocean tsunami: Kirinda Harbor, Sri Lanka. *Geomorphology* 127, 107–116.
- Hoffmann, N., Master, D., Goodman-Tchernov, B., 2018. Possible tsunami inundation identified amongst 4–5th century BCE archaeological deposits at Tel Ashkelon, Israel. *Marine Geology* 396, 150–159.
- Jaffe, B., Gelfenbaum, G., Rubin, D., Peters, R., Anima, R., Swenson, M., Olcese, D., Anticona, L.B., Gomez, J.C., Riega, P.C., 2003. Identification and interpretation of tsunami deposits from the June 23, 2001 Perú tsunami. *Coastal Sediments 2003 Conference Proceedings*.
- Katz, O., Mushkin, A., 2013. Characteristics of sea-cliff erosion induced by a strong winter storm in the eastern Mediterranean. *Quaternary Research* 80, 20–32.
- Katz, O., Reuven, E., Aharonov, E., 2015. Submarine landslides and fault scarps along the eastern Mediterranean Israeli continental-slope. *Marine Geology* 369, 100–115.
- Klein, M., Zviely, D., Kit, E., Shteinman, B., 2007. Sediment transport along the Coast of Israel: examination of fluorescent sand tracers. *Journal of Coastal Research* 23, 1462–1470.
- Kortekaas, S., Dawson, A.G., 2007. Distinguishing tsunami and storm deposits: an example from Martinhal, SW Portugal. *Sedimentary Geology* 200, 208–221.
- Lambeck, K., Rouby, H., Purcell, A., Sun, Y., Sambridge, M., 2014. Sea level and global ice volumes from the last glacial maximum to the Holocene. *Proceedings of the National Academy of Sciences* 111, 15296–15303.
- Maramai, A., Brizuela, B., Graziani, L., 2014. The Euro-Mediterranean tsunami catalogue. *Annals of Geophysics* 57, S0435.
- Moore, A.L., Brian G. McAdoo, B.G., Ruffman, A., 2007. Landward fining from multiple sources in a sand sheet deposited by the 1929 Grand Banks tsunami, Newfoundland. *Sedimentary Geology* 200, 336–346.
- Morton, R.A., Gelfenbaum, G., Jaffe, B.E., 2007. Physical criteria for distinguishing sandy tsunami and storm deposits using modern examples. *Sedimentary Geology* 200, 184–207.
- Negev, A., Gibson, S., 2001. *Archaeological Encyclopedia of the Holy Land*. New York and London, Continuum, pp. 25–26.
- Nelson, A.R., Briggs, R.W., Dura, T., Engelhart, S.E., Gelfenbaum, G., Bradley, L., Forman, S.L., Vane, C.H., Kelley, K.A., 2015. Tsunami recurrence in the eastern Alaska-Aleutian arc: a Holocene stratigraphic record from Chirikof Island, Alaska. *Geosphere* 11, 1172–1203.
- Papadopoulos, G.A., Gràcia, E., Urgeles, R., Sallares, V., De Martini, P.M., Pantosti, D., González, M., Yalciner, A.C., Mascle, J., Sakellariou, D., Salamon, A., Tinti, S., Karastathis, V., Fokaefs, A., Camerlenghi, A., Novikova, T., Papageorgiou, A., 2014. Historical and pre-historical tsunamis in the Mediterranean and its connected seas: geological signatures, generation mechanisms and coastal impacts. *Marine Geology* 354, 81–109.
- Paris, R., Fournier, J., Poizot, E., Etienne, S., Morin, J., Lavigne, F., Wassmer, P., 2010. Boulder and fine sediment transport and deposition by the 2004 tsunami in Lhok Nga (western Banda Aceh, Sumatra, Indonesia): a coupled offshore-onshore model. *Marine Geology* 268, 43–54.
- Peters, R., Jaffe, B., Gelfenbaum, G., 2007. Distribution and sedimentary characteristics of tsunami deposits along the Cascadia margin of western North America. *Sedimentary Geology* 200, 372–386.
- Pfannenstiel, M., 1952. *Das Quartaer der Levante, I: Die Kueste Palaestina-Syriens*, Akad. In: *Abhandlungen Der Mathematisch-Naturwissenschaftlichen Klasse, Akademider Wissenschaften Und Der Literatur in Mainz in Kommission Bei F. Steiner*, pp. 373–475.
- Pfannenstiel, M., 1960. Erläuterungen zu den bathymetrischen Karten des östlichen Mittelmeeres. *Bulletin de l’Institut Océanographique* 1192, 1–60.
- Phantuwongraj, S., Choowong, M., 2012. Tsunamis versus storm deposits from Thailand. *Natural Hazards* 63, 31–50.
- Pilarczyk, J.E., Dura, T., Horton, B.P., Engelhart, S.E., Kemp, A.C., Sawai, Y., 2014. Microfossils from coastal environments as indicators of paleo-earthquakes, tsunamis and storms. *Palaeogeography, Palaeoclimatology, Palaeoecology* 413, 144–157.
- Rosen, A., 2008. Site formation. In: Stager, L., Schloen, D.J., Master, D. (Eds.), *Ashkelon 1: Introduction and Overview*. Eisenbrauns, Winona Lake, Indiana, pp. 101–104.
- Sakuna-Schwartz, D., Feldens, P., Schwarzer, K., Khokiattiwong, S., Stattegger, K., 2015. Internal structure of event layers preserved on the Andaman Sea continental shelf, Thailand: tsunami vs. storm and flash-flood deposits. *Natural Hazards and Earth System Sciences* 15, 1181–1199.
- Salamon, A., Rockwell, T., Guidoboni, E., Comastri, A., 2011. A critical evaluation of tsunami records reported for the Levant coast from the second millennium BCE to the present. *Israel Journal of Earth Sciences* 58, 327–354.
- Salamon, A., Rockwell, T., Ward, S.N., Guidoboni, E., Comastri, A., 2007. Tsunami hazard evaluation of the Eastern Mediterranean: historical analysis and selected modeling. *Bulletin of the Seismological Society of America* 97, 705–724.
- Scheffers, A.M., 2002. Paleotsunami evidences from boulder deposits. *Science of Tsunami Hazards* 20, 26–37.
- Scheucher, L.E.A., Vortisch, W., 2011. Sedimentological and geomorphological effects of the Sumatra-Andaman tsunami in the area of Khao Lak, southern Thailand. *Environmental Earth Sciences* 63, 785–796.
- Shah-Hosseini, M., Morhange, C., De Marco, A., Wante, J., Anthony, E.J., Sabatier, F., Mastronuzzi, G., Pignatelli, C., Piscitelli, A., 2013. Coastal boulders in Martigues, French Mediterranean: evidence for extreme storm waves during the Little Ice Age. *Zeitschrift für Geomorphologie, Supplementary Issues* 57 (4), 181–199.

- Sivan, D., Wdowinski, S., Lambeck, K., Galili, E., Raban, A., 2001. Holocene sea-level changes along the Mediterranean coast of Israel, based on archaeological observations and numerical model. *Palaeogeography, Palaeoclimatology, Palaeoecology* 167, 101–117.
- Sivan, D., Lambeck, K., Toueg, R., Raban, A., Porath, Y., Shirman, B., 2004. Ancient coastal wells of Caesarea Maritima, Israel, an indicator for relative sea level changes during the last 2000 years. *Earth and Planetary Science Letters* 222, 315–330.
- Soloviev, S.L., Solovieva, O.N., Go, C.N., Kim, K.S., Shchetnikov, N.A., 2000. *Tsunamis in the Mediterranean Sea 2000 BC–2000 AD*. Kluwer Academic Publishers, Dordrecht, pp. 239.
- Ubeid, K.F., 2016. Quaternary Stratigraphy Architecture and Sedimentology of Gaza and Middle- to Khan Younis Governorates (The Gaza Strip, Palestine). *International Journal of Scientific and Research Publications* 6, 109–117.
- Ubeid, K.F., 2010. Marine lithofacies and depositional zones analysis along coastal ridge in Gaza Strip, Palestine. *Journal of Geography and Geology* 2, 68–76.
- Ubeid, K.F., 2011. Sand Characteristics and Beach Profiles of the Coast of Gaza Strip, Palestine. *Serie Correlacion Geologica* 27, 121–132.
- Ubeid, K.F., Al-Agha, M.R., Almeshal, W.I., 2018. Assessment of heavy metals pollution in marine surface sediments of Gaza Strip, southeast Mediterranean Sea. *Journal of Mediterranean Earth Sciences* 10, 109–121.
- Ubeid, K.F., Albatta, A., 2014. Sand dunes of the Gaza Strip (southwestern Palestine): morphology, textural characteristics and associated environmental impacts. *Earth Sciences Research Journal* 18, 131–142.
- Ubeid, K.F., Ramadan, K.A., 2017. Activity concentration and spatial distribution of radon in beach sands of Gaza Strip, Palestine. *Journal of Mediterranean Earth Sciences* 9, 19–28.
- Weiss, R., 2012. The mystery of boulders moved by tsunamis and storms. *Marine Geology* 295, 28–33.
- Yolsal, S., Taymaz, T., Yalc, Iner, A.C., 2007. Understanding tsunamis, potential source regions and tsunami-prone mechanisms in the Eastern Mediterranean. *Geological Society London Special Publications* 291, 201–230.
- Zainali, A., Weiss, R., 2015. Boulder dislodgement and transport by solitary waves: insights from three-dimensional numerical simulations. *Geophysical Research Letters* 42, 4490–4497.
- Zviely D., Kit E., Klein M., 2007. Longshore sand transport estimates along the Mediterranean coast of Israel in the Holocene. *Marine Geology* 238, 61–73.